Very Low-Pressure Pyrolysis. I. Kinetic Studies of Homogeneous Reactions at the Molecular Level

Sidney W. Benson and G. Neil Spokes

Contribution from the Department of Thermochemistry and Chemical Kinetics, Stanford Research Institute, Menlo Park, California. *Received September 19, 1966*

Abstract: Gases have been pyrolyzed in a very low-pressure environment in which attention has been given to the establishment of uniform temperature conditions, and energy transfer is predominantly *via* gas–wall collisions. We have compared the observed low-pressure and theoretical high-pressure decomposition rates of molecules of widely different chemical and structural character. Complicated molecules with small activation energies are pyrolyzed into simpler products at a rate which is close to the high-pressure rate. Simpler molecules decompose more slowly at rates which become controlled by energy transfer. Wall catalysis is relatively unimportant in the process. Studies of the unimolecular decomposition of isopropyl iodide have given information on: (1) the energy accommodation between wall and molecule, (2) the effective number of Kassel oscillators deduced from a simple theoretical treatment of the data, and (3) the effects of wall conditioning on the decomposition rate. The kinetic equations for the steady-state condition in a stirred flow reactor at very low pressures are evaluated explicitly. These include the effects of induction periods due to "mixing" and to lack of attainment of a steady-state internal energy distribution. Preliminary results on isopropyl iodide indicate that about 80 wall collisions are needed to attain steady state at 900°K.

A number of authors[1-6] have pyrolyzed complex molecules at sufficiently low pressures that there are very few gas-phase collisions, and most collisions take place with the walls of the vessels. The results of such studies have been useful as a means of producing free radicals and, in one or two isolated instances, they have given information about the initial molecular fission or isomerization. However, quantitative interpretation of the kinetics has proven difficult. Numerous reasons can be cited for this difficulty, but the principal reasons have been that the Boltzmann equilibrium has not been achieved in the reacting gas and that the wrong equations have been applied to the results and have resulted in incorrect interpretation of the data. It is the purpose of the present and succeeding papers to describe a variant of these experimental techniques which lends itself to quantitative interpretation and thus provides a new kinetic tool for the quantitative study of the details of unimolecular reactions, energy transfer, and bimolecular reactions in the gas phase. It can also be used to study heterogeneous reactions.[7] It is useful to refer to the technique as "very low-pressure pyrolysis" or "VLPP."

Experimental Section

Apparatus and Procedure. The gas to be studied is stored in a 5-l. reservoir at a few torr pressure. The gas passes through an adjustable leak valve at a rate of from 10^{15} to 10^{16} molecules/sec and into the reactor through a short length of small bore capillary tube which prevents back diffusion from the reactor. Pyrolysis occurs in a cylindrical fused silica reactor approximately 9 cm long and 2.2 cm i.d. The ratio of internal surface area to exit aperture area gives the average number of gas–wall collisions Z_r made by a molecule while in the reactor. We have a number of reactors whose exit apertures are in the range of 0.8 to 0.008 cm². A typical vessel is shown in Figure 1. A pair of 1-cm² fused silica baffles interrupt the direct path between the gas injection capillaries and the exit aperture. The pyrolysis vessel temperature is maintained to better than ±10° up to 1000°. Heating is by means of a pair of 4-in. long clam shell heaters[8] with temperature "trimming" elements (each consisting of a coil of nichrome heating element) placed at the upper and lower parts of the furnace. Six chromel–alumel thermocouples monitor temperature at various parts of the vessel. The low thermal inertia system is lagged with Microquartz fiber to exclude drafts. (Microquartz[9] is a fabric composed of short, fine, quartz fibers; its properties are essentially unaffected by a Bunsen flame.) We have arranged for a sharp temperature gradient at the point of gas injection in order to heat the injected molecules as fast as possible. It is very important to avoid pyrolysis of the gas in the higher pressure region above this injection capillary. Gas density in the reactor depends on the area of the pyrolysis chamber exit aperture, on the degree of molecular decomposition achieved, and on factors such as molecular throughput, temperature, and molecular weight.

Gases which effuse from the reactor pass to the ionization chamber of a quadrupole mass spectrometer.[10] A schematic drawing of the apparatus is given in Figure 2. The spectrometer is located in a large (10-in. i.d. by 18-in. long) cylindrical aluminum chamber. Electrical connections are made by means of Kovar glass seals which are epoxied (using Epon 828 vacuum epoxy) to the aluminum support plate. An NRC HS4-750 pump (5-in. diffusion pump), using DC704 pump oil, evacuates the chamber through an ambient-cooled baffle and a 4-in. Temescal manifold gate valve. The base pressure of the system is about 10^{-6} torr; a slight air leak gives peaks at 28 and 32 amu, and other residual gases give interference at 17, 18, 73, 77, 78, 91, and 135 amu and, less importantly, at numerous other places in the mass spectrum. A correction is applied when interference occurs. Ordinarily such interference is serious only when H_2O, O_2, or N_2 are produced and have to be measured explicitly. The effective pumping speed is about 60–80 l./sec in the

(1) E. J. Sinke, G. A. Pressley, A. B. Baylis, and F. E. Stafford, *J. Chem. Phys.*, 41, 2207 (1964); A. B. Baylis, G. A. Pressley, Jr., and F. E. Stafford, *J. Am. Chem. Soc.*, 88, 2428 (1966).

(2) P. LeGoff, A. Cassuto, and A. Pentenero, *Ind. Chim. Belge*, 29 (4), 342 (1964); paper presented at the 12th ASTM Conference on Mass Spectrometry and Allied Topics, Montreal, Canada, 1964.

(3) I. P. Fisher, J. B. Homer, B. Roberts, and F. P. Lossing, material presented at the Ottawa Symposium on Pyrolysis, Sept 1964. They used a He carrier to produce high space velocities and thus had many He reactive gas collisions but almost no secondary reactions.

(4) T. F. Thomas and D. F. Swinehart, 150th National Meeting of the American Chemical Society, Atlantic City, N. J., Sept 1965, p 65-V.

(5) T. P. Fehlner and W. S. Koski, *J. Am. Chem. Soc.*, 87, 409 (1965).

(6) J. Collin, "Pyrolysis Studies by Mass Spectrometry," EUR2114e—Euratom Report obtainable from Presses Academiques Europeennes, 98 Chaussée de Charleroi, Brussels 6.

(7) J. D. McKinley, *J. Chem. Phys.*, 40, 120 (1964).

(8) Hevi Duty Type 73 KS designed for operation at up to 1200° with 210-w input power, manufactured by the Hevi Duty Electric Co., Watertown, Wis.

(9) Obtainable from Western Asbestos Co., Brisbane, Calif. 94005.

(10) Further details regarding the operating characteristics of the mass spectrometer will be supplied by the authors on request.

mass spectrometer chamber. The mass spectrometer consists of an ionizer, rod system, and particle multiplier tube fed by appropriate power supplies. Data are recorded by an oscilloscope–Polaroid camera combination.

The electronics which supply the quadrupole analyzer rods were designed by members of the Engineering Department of Stanford Research Institute.[11] The radiofrequency generator operates at a fixed frequency, and the mass spectrum is scanned by variation of applied voltage. A sawtooth signal from a waveform generator (Tektronix, Type 162) drives a dc amplifier and a coupled radio-frequency generator and, in addition, the signal drives or triggers

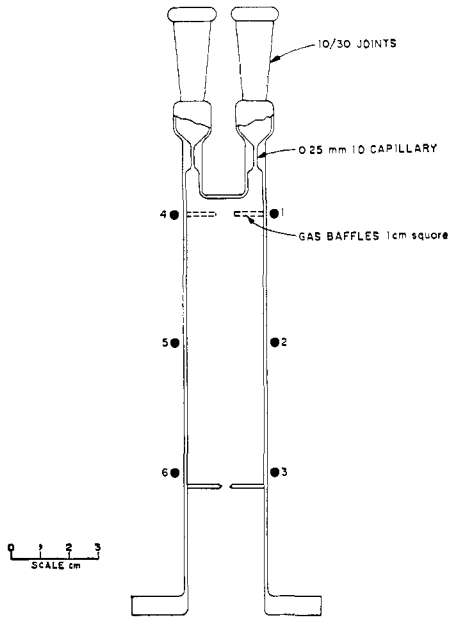

Figure 1. Very low-pressure pyrolysis fused silica reactor. Thermocouple locations are indicated by the numbers 1–6.

the horizontal sweep of the recording oscilloscope (Tektronix 535A). Linearity of mass-filtered *vs.* instantaneous voltage of the sawtooth gives a linear mass spectrum on the oscilloscope screen. The radiofrequency/dc ratio has to be maintained accurately in order to obtain a stable mass spectrum. Under normal operating conditions the electrical inputs to the analyzer rod system are adjusted until we get a mass spectrum whose relative peak heights are almost unchanged as the radiofrequency/dc ratio control (or resolution) is changed.

We have found it necessary to keep the electronics running at constant sweep rate in order to avoid drift effects[12] which appear when the quadrupole electronics are operated at fixed output (*i.e.*, when attempting to measure the intensity of a single peak). This has so far limited our precision to about ±5%. We have found that best accuracy can be achieved by measuring adjacent or close-spaced mass peaks. For this reason, for example, work on *i*-PrI decomposition to C_3H_6 and HI has been followed most easily by monitoring the peaks 39, 40, 41, 42, and 43. We think that our analytical methods cause errors of less than about 5% (in midrange) in the rate constants.[13]

For the work reported in this paper, no effective trapping had been provided between the diffusion pump and the mass spectrometer. It was thus necessary to heat the ionizer to a temperature of about 200° in order to maintain ionizer operation for as long as several days.

The ionizer is mounted approximately 7 cm from the furnace exit aperture. We estimate that less than 1.6% of the gas concentration in the ionizer is due to species which have arrived there from the reactor without making any collisions. The electron beam is directed at right angles to the analyzer rod system axis. Typically, operating pressures in the spectrometer chamber are below 10^{-6} torr, and satisfactory signals are obtained with an electron beam current of about 2 ma at 70 ev. Interruption of the path between

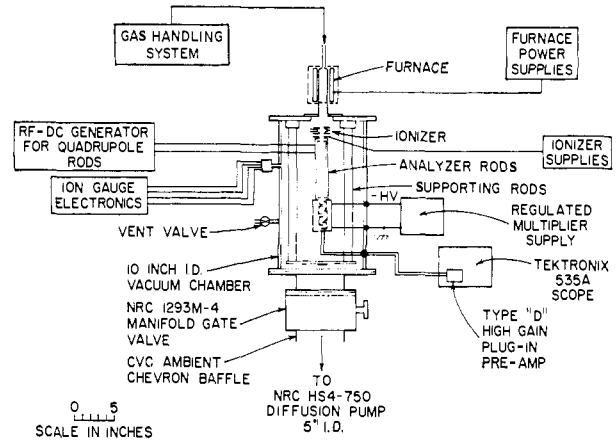

Figure 2. Schematic of low-pressure pyrolysis apparatus.

furnace and ionizer by means of a beam flag has shown that only about 15–30% of the signal of the detector is due to gases which have just emerged from the reactor into the volume between the reactor exit aperture and the ionizer. These gas molecules will have already made a number of collisions with walls in the neighborhood of this volume. The bulk of the signal is given by gases which have made many collisions with the walls of the spectrometer chamber and have thus cooled to a low temperature. We do not, therefore, make any $(T/M)^{1/2}$ correcton to adjust for changing sensitivities for substances of different mass.

We have also noted that after a rapid change is made in the nature of the gases injected into the mass spectrometer, the spectrum may take some minutes to readjust to its new values. For example, when equimolar amounts of *i*-C_3H_7I and C_3H_6 are injected, several minutes must elapse after their introduction before reproducible runs are obtained. Similarly, when furnace temperature is raised so that the amount of decomposition is changed appreciably, a waiting time must be allowed for equilibration.

Some free-radical products such as CH_3 cannot be detected directly with the present instrument, although their presence has been established by titration with NO_2. We are well aware of the problems attaching to direct detection of free radicals with mass spectrometers[14] and have not attempted to surmount them in this work.

Results

A. Pyrolysis of Selected Compounds. The extent of decomposition of the reactant listed in Table I was followed by measuring the ratio of reactant peaks to product peaks. Where available, API[15] sensitivity data were used to estimate decomposition. When they were not available, estimates were made from the re-

(11) We are grateful to members of the Applied Physics group of Stanford Research Institute for the use of their designs of various parts of the quadrupole spectrometer and electronics.

(12) These drift effects seem to have been eliminated in a new set of electronics recently acquired from Electronic Associates Inc., Palo Alto, Calif.

(13) Other errors such as the determination of the escape rate constant of the reactor are comparable with this. A referee has pointed out that perhaps 10% of the material emerging from a 100-collision reactor will reenter the vessel and be subjected to further pyrolysis. All quoted rates for reactors of 93, 110, and 120 collisions should be reduced by about 10%.

(14) F. P. Lossing in "Mass Spectrometry," C. A. McDowell, Ed., McGraw-Hill Book Co., Inc., New York, N. Y., 1963, p 442.

(15) American Petroleum Institute Project 44, Collection of Mass Spectral Data, Carnegie Institute of Technology, Pittsburgh, Pa., June 30, 1959.

Table I. Comparison of VLPP Data for Some Selected Compounds with High-Pressure Rates,[a] Nominal 110-Collision Vessel

Reaction	Log k_∞[b]	T_{20}	k_u^{20}	k_∞^{20}	T_{60}	k_u^{60}	k_∞^{60}
$CH_3I \rightarrow CH_3 + I$	$14.5-56/\theta$[c]	>1100	<44	>2500	>1100		
$CHCl_3 \rightarrow CCl_2 + HCl$	$11.4-47/\theta$[d]	>1370	<53.5	>8000	>1370		
$CH_3CCl_3 \rightarrow CH_2CCl_2 + HCl$	$14.0-54/\theta$[e]	~1370	50.6	2.5×10^5	>1370	<303	$>2.5 \times 10^5$
n-$C_3H_7Cl \rightarrow C_3H_6 + HCl$	$13.0-54/\theta$	~1270	63.6	5000	>1370	<365	$>2.4 \times 10^4$
i-$C_3H_7I \rightarrow C_3H_6 + HI$	$13.0-43.5/\theta$	1070	39.6	1.3×10^4	1220	254	1.6×10^5
$CH_3COOEt \rightarrow CH_3COOH + C_2H_4$	$12.0-46/\theta$	~1020	53.8	215	~1120	338	1000
t-$BuOH \rightarrow i$-$C_4H_8 + HOH$	$13.5-60/\theta$	~1120	61.6	63	~1220	385	630
toluene $\rightarrow C_6H_5CH_2\cdot + H$	$14.8-84/\theta$[f]	>1370	<61.0	>25	>1370		
$(C_5H_6)_2 \rightarrow 2C_5H_6$[h]	$13.0-33.7/\theta$	~620	34.2	13	~730	223	830
$[(CH_3)_3CO]_2 \rightarrow 2(CH_3)_3CO$	$15.6-37.5/\theta$[g]	~620	32.6	240	~690	195	6300

[a] Literature values of Arrhenius parameters are given in the second column. The temperatures (or their limits) at which 20 and 60% decomposition was observed are listed in the columns headed T_{20} and T_{60}. The terms k_u^{20} and k_u^{60} are the apparent first-order rate constants at T_{20} and T_{60}. (From the stirred flow reactor equations we have $k_u^{20} = 0.2(1 - 0.2)^{-1}k_{ea}$, where k_{ea} is the escape rate constant for the reactor.) The terms k_∞^{20} and k_∞^{60} are high-pressure rate constants at T_{20} and T_{60}, respectively. The ratio of k_u to k_∞ gives a measure of the fall-off. [b] Arrhenius parameters taken from compilation by S. W. Benson, "Foundations of Chemical Kinetics," McGraw-Hill Book Co., Inc., New York, N. Y., 1960. Units are sec^{-1} for all rate constants. [c] Estimated from back-reaction and thermal data. $\theta = 2.303RT$ in kcal/mole. [d] A. E. Shilov and R. D. Sabirova, *Russ. J. Phys. Chem.*, **34**, 408 (1960). [e] D. H. R. Barton and P. F. Onyon, *J. Am. Chem. Soc.*, **72**, 988 (1950). [f] S. J. Price, *Can. J. Chem.*, **40**, 1310 (1962). [g] L. Batt and S. W. Benson, *J. Chem. Phys.*, **36**, 895 (1962). [h] C_5H_6 = 1,3-cyclopentadiene.

duction in parent peak intensity, using eq 17 of the Appendix. Species like di-t-butyl peroxide give unstable t-BuO radicals, which decompose completely in our system to acetone + CH_3. This makes them useful as sources of CH_3 radicals. Extent of decomposition was determined from measurement of the ratio of mass peaks at 146 and 73 amu (parent compound) to that at 58 amu (acetone). Preliminary data on some of the reactions we have studied in a nominal 110-collision vessel are shown in Table I. Rather than give the entire decomposition curves, we have listed the temperatures at which we have observed 20 and 60% decomposition. For comparison we have given the high-pressure rate constants, using literature values for the Arrhenius parameters. We have used the equations for a stirred flow reactor to derive the apparent first-order rate constants from the per cent reaction. Details of the application of these equations to our system are developed in the Appendix.

In the cases of CH_3I, $CHCl_3$, and toluene, we observed no measurable decomposition in this vessel up to the highest temperatures listed.

The mean molecular residence time in the vessel was about $16(M/T)^{1/2}$ msec, where M is the mass in amu. For i-PrI, for example, this was about 6.5 msec at 1000°K.

B. Isopropyl Iodide. In order to check the validity of the results of VLPP for measurements of kinetics and energy exchange, we have studied the unimolecular decomposition of i-PrI in a number of vessels of different nominal collision numbers.

The unimolecular decomposition of isopropyl iodide and the inverse reaction (addition of HI to propene) have been thoroughly investigated by several groups of workers, and there is satisfactory agreement on the rate constants of the reactions.[16,17] For reaction i, $k_\infty = 10^{12.96-43.5/\theta}$ sec^{-1}, where $\theta = 2.303RT$ (kcal/mole).

$$i\text{-}C_3H_7I \longrightarrow C_3H_6 + HI \qquad \text{(i)}$$

The error limits on log A_1 are ±0.5 and on E are ±1.0 kcal/mole; k_∞ refers to the high-pressure rate constant.

Isopropyl iodide was pyrolyzed in our fused silica vessels at very low pressures. Gas flows were typically 3×10^{15} to 5×10^{15} molecules sec^{-1}; except for the 9000-collision vessel, molecules made very many more collisions with the wall than with other molecules. For the 9000-collision reactor the mean free path for gas–gas collision was 4 cm compared with about 2 cm for gas–wall collisions. The decomposition rate was measured as a function of temperature for several vessels whose collision numbers Z_r were 93, 110, 630, 1100, and 9000.[18] The relative heights of the fragment peaks at 43 and 41 amu give an accurate measure of the amount of decomposition. These mass peak heights were measured after steady state had been reached at each temperature. The fraction of undecomposed material was calculated from our measurements of the relative sensitivities of these peaks, the parent compound, and propylene. (There is a small but important contribution to the 43 peak from C^{13}-$C^{12}{}_2H_6^+$.) A slight error is introduced into our results, since we cannot be sure that parent molecules will contribute to peaks 43 and 41 in the same way when the furnace is at a high temperature as they do when it is cold. This error could be significant when decomposition is less than 5%, but the approximation which ignores this correction should be satisfactory when decomposition is in excess of this amount.

From the kinetic equations which have been derived for the VLPP conditions, we compute apparent first-order rate constants $k = k_e\delta$, where δ is the ratio of product to reactant fluxes and k_e is the known first-order rate constant for escape from our reactor.[19] Figure 3 shows log k as a function of temperature for the different reactors (k is in sec^{-1}). Included for comparison is k_∞ calculated from the Arrhenius parameters.

Individual points in Figure 3 are averages of three or more observations. Each observation was made

(16) H. Teranishi and S. W. Benson, *J. Chem. Phys.*, **40**, 2946 (1964); S. W. Benson and A. N. Bose, *ibid.*, **37**, 1081 (1962).
(17) W. Tsang, *ibid.*, **41**, 2487 (1964), and references cited therein.

(18) Collision number is given by the ratio of internal surface area to exit aperture area. All vessels were cylinders of 2.2 cm internal diameter and length about 9 cm.

(19) We estimate that for i-PrI in our vessels, $k_e = 8.5A_h\sqrt{T}$ sec^{-1}, where A_h cm^2 is the exit aperture area.

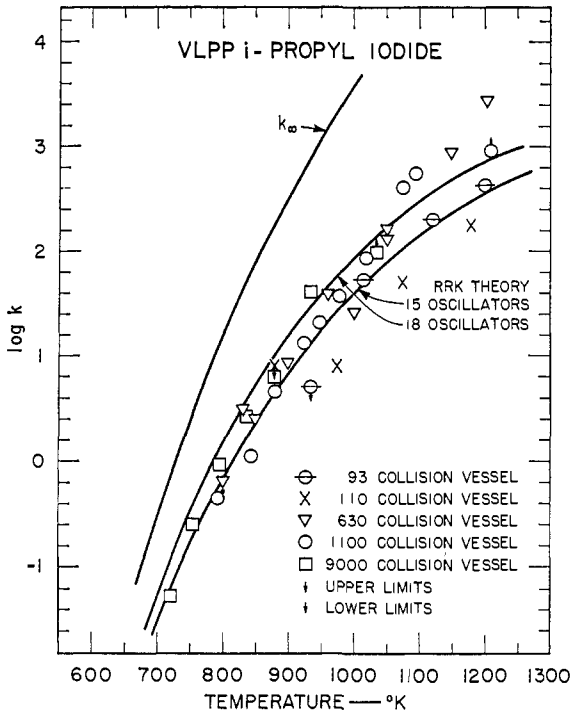

Figure 3. Apparent first-order rate constant for isopropyl iodide decomposition. The dimensions of k are sec^{-1}.

after short-term (*i.e.*, ~15 min) reproducibility was obtained. Long-term (*i.e.*, on a day-to-day basis) reproducibility was generally fairly good on well-conditioned vessels. These included the 110-, 1100-, and 9000-collision reactors. The effect of history is illustrated for the less well-conditioned 630-collision reactor. Reactor temperature (°K) was increased in steps as follows: 300, 700, 800, 830, 898, 958, 1000, 1050, again 1050 after 90 min at temperature, 1148, and 1203. The temperature was then reduced to 1000 and then to 848°K. (Except for the second run at 1050°K, readings were ordinarily taken after 15 min at temperature.) Results for the 93-collision vessel are included for interest, although this reactor was previously unused. No conditioning studies were possible with this reactor, since it broke during a run at 1300°K. Its "freshness" could account for the apparently fast rates compared with the 110-collision reactor.

A well-conditioned vessel differs visually from a fresh one; it is slightly darker in color. HF solution acts on the walls, causing a thin, dark (presumably carbonaceous) film to peel off. We have estimated that the percentage of material decomposing *via* carbon and other products is less than 10%.

Discussion

The high-pressure rate constants approximately describe the observed results for the more complex molecules but are inadequate for the simpler ones in the 110-collision vessel. Further confirmatory work is required to clarify some of the data, particularly the fate of the radical species in the case of di-*t*-butyl peroxide decomposition. It is clear from the slowness of the rates found from the experimental data that the walls are not "catalyzing" the reactions of the reactant molecules listed in Table I. The principal value of the work on the pyrolysis of this wide range of compounds was to eliminate our fear that wall reactions would seriously interfere with the pyrolysis. However, we would like to know the magnitudes of the relative roles of low-pressure falloff effects and of slowness of energy equilibration, for example. We have some indication of the importance of the latter process for *i*-PrI, but a comprehensive survey of all of these molecules would be of considerable general interest.

In order to unravel the various kinetic features from one another, we have developed, in the Appendix, a treatment of the theory of the method which we think is able to explain the data quantitatively.

Comparison of k_∞ for *i*-PrI with the observed rates confirms that energy transfer to the molecules limits the rate of decomposition.

Equations derived from the theory in the Appendix permit us to evaluate k from the classical Arrhenius parameters and from n, the effective number of internal oscillators in *i*-PrI. These theoretical values are shown in Figure 3 for $n = 15$ and 18 and appear to bracket the experimental data very well except at the highest temperatures. It may be that the precision of our data warrants the more accurate RRKM[20] quantum theory, and we are exploring this possibility.

The difference in the rate constants for the 110- and for the 630- and 1100-collision vessels arises from the slowness of energy accommodation between wall and molecule which introduces an induction period, appreciable only for the smaller collision-number reactors. At 900°K the energy required by an *i*-PrI molecule to undergo breakup in about $10^{-4.3}$ sec is of the order of 60 kcal/mole or $\sim 30RT$. Accommodation to this energy seems to occur in 80 ± 30 collisions.[21]

Wall-conditioning appears to be associated with the formation of a carbonaceous coating. The conditioning process could be associated with different energy-transfer processes between wall and reactant as the wall is progressively coated. The alternative view which cannot yet be ruled out is that the wall gives rise to catalytic decomposition of parent molecules. The occurrence of coating obviously implies that wall-promoted reactions can occur. Their rates are small, however, on our time scale, and it is more likely that these reactions are taking place with products than with reactants.

We are continuing our investigations of the nature of wall-conditioning effects and will report on these subsequently.

Application of the Method

The possible applications of the low-pressure pyrolysis technique to chemical kinetics are manifold. By covering a large temperature range, we are able to measure apparent unimolecular rate constants k_d whose values range in each case over 4 to 6 decades (*e.g.*, $10^{-2} < k_d < 10^{3.5}$ sec^{-1}). For most molecules studied, this carries k into the region well below the high-pressure limit rate constant k_∞, and energy trans-

(20) D. W. Placzek, B. S. Rabinovitch, G. Z. Whitten, and E. Tschuikow-Roux, *J. Chem. Phys.*, 43, 4071 (1965).
(21) Calculated from theory presented in Appendix, eq 24.

fer is rate controlling. Using the theory with the experimental data, it is possible to obtain the Arrhenius parameters for k_∞ and the details of energy transfer, either with the walls or with added carrier gases. Studies of the induction times in low-collision-number vessels yield values for the rates at which the upper vibrational levels of complex molecules relax in collisions. Such studies are now under way.

Perhaps the most important use for VLPP is in the study of the direct products of primary thermal excitation in unimolecular decomposition. Thus we have found that both 1- and 2-nitropropane decompose to give[22] $C_3H_6 + HNO_2$, rather than the much discussed *n*- or isopropyl radical + NO_2. We hope to distinguish the paths $CHCl_3 \rightarrow CHCl_2 + Cl$ (or $CCl_2 + HCl$) in $CHCl_3$ pyrolysis. Present data[23] indicate that carbene formation is important. We estimate that the activation energy exceeds 56 kcal.[24]

Finally, the system lends itself extremely well to direct studies of the kinetics and stoichiometry of molecule–surface reactions, and we are now beginning studies of this type for suitable molecules with various graphitic and metal surfaces.

Appendix. Treatment of Data

The experimental technique of very low-pressure pyrolysis (VLPP)[25] consists of permitting a steady-state flow of reactant molecules to pass into a thermostated reaction cell under conditions of such low pressure that most collisions of reactant (or product) molecules take place with the vessel walls and not in the gas phase. For our usual reactors this corresponds to pressures $P \leq 10^{-2}$ torr. Once in the cell, reactant molecules may decompose, escape from the cell, or, in special cases, react chemically with added carrier gases or products. In conditioned quartz vessels, the rates of heterogeneous reactions have turned out to be small (*i.e.*, less than 10% of the observed rates). This is not necessarily the case in metal vessels.

The apparent first-order rate constants measured in our system fall considerably below those obtained at higher pressures in static systems. In the following sections we shall develop the appropriate equations which permit us to interpret our data and explain quantitatively the falloff in rate constants in our system and in similar ones.

1. Flow Kinetics. The conditions in VLPP correspond closely to those in a stirred flow reactor.[26,27] An important difference between the usual stirred flow reactor equation and those applicable here will emerge shortly. We can represent the mechanism by the following set of kinetic equations in which A represents a reactant molecule and B represents an added carrier species (*e.g.*, NO_2) or product molecule which can react with A (or the products of A).

$$\begin{array}{l} \mathrm{A} \xrightarrow{k} \text{products } [n_p\mathrm{P} + n_q\mathrm{Q}] \\ \mathrm{A} \xrightarrow{k_{ea}} \text{escape through orifice} \\ \mathrm{A} + \mathrm{B} \xrightarrow{k_b} \text{other products } [n_r\mathrm{R} + n_s\mathrm{S}] \end{array} \quad (1)$$

where n_i is the stoichiometric number of moles of product formed per mole of A decomposing.

$(A)_{SS}$, the steady-state concentration of A in the reactor, is determined by the rate of introduction N_A in moles/second (essentially the steady-state flow rate) and the various depletion processes. From the above we find

$$(A)_{SS} = \frac{N_A}{[k_{ea} + k + k_b(B)_{SS}]V} \quad (2)$$

where V is the reactor volume in liters and concentrations are in units of moles/liter. The steady-state concentration of species in the reactor thus depends on k_{ea} and $k_b(B)_{SS}$. These terms depend in turn on an average molecular speed, and there is thus this important difference between the stirred flow reactor equations for high and for very low pressures.

The flux of unreacted A in the exit stream is given by

$$Vk_{ea}(A)_{SS} = \frac{N_A k_{ea}}{[k_{ea} + k + k_b(B)_{SS}]} \quad (3)$$

The exit flux of product molecules P at steady state is

$$Vk_{ep}(P)_{SS} = k(A)_{SS} n_p V \quad (4)$$

where k_{ep} is the first-order escape rate constant for P.

The mass spectrometer is calibrated by passing known fluxes of products and reactants through the system. From the observed signals at two or more mass peaks, we can determine the relative fluxes of product and reactant. From eq 4, this relative flux δ_p or δ_q for product P or Q is given by

$$\delta_p = \frac{k_{ep}(P)_{SS}}{k_{ea}(A)_{SS}} = \frac{kn_p}{k_{ea}} \quad (5)$$

$$\delta_q = \frac{k_{eq}(Q)_{SS}}{k_{ea}(A)_{SS}} = \frac{kn_q}{k_{ea}} \quad (6)$$

where δ_p and δ_q are the ratios of the observed signals of P and Q, respectively, to A. We can write similar equations for δ_r and δ_s, the relative fluxes of R and S. From kinetic theory[28] the escape rate constant through a thin aperture is[29]

$$k_{ea} = \frac{{}^1/_4 \bar{c}_A A_h}{10^3 V} \text{ sec}^{-1} \quad (7)$$

where A_h is the hole area in cm^2 and $\bar{c}_A$ is the mean molecular speed of A. From kinetic theory $\bar{c}_A = 1.46 \times 10^4 (T/M_A)^{1/2}$ cm/sec. M_A is the mass of A in amu. Hence, from eq 5 and 7

$$k = \frac{3.65 A_h \delta_p T^{1/2}}{V n_p M_A^{1/2}} \quad (8)$$

Using the relation $Z_r = A_v/A_h$, we can, if we wish,

(22) G. N. Spokes and S. W. Benson, manuscript in preparation.
(23) S. W. Benson and G. N. Spokes, paper submitted to the 11th Symposium on Combustion, Berkeley, Calif, Aug 1966.
(24) Assuming an A factor of $10^{13.5}$ sec^{-1} and a Kassel n of 7.5.
(25) VLPP may be defined as "pyrolysis in a reactor at low pressure such that energy transfer from an external heat source is primarily by means of gas–wall interactions. Gas flow is chiefly free molecular flow. Temperature history of average molecules is well characterized."
(26) M. Bodenstein and K. Wolgast, *Z. Physik. Chem.*, 61, 422 (1908).
(27) K. Denbigh, "Chemical Reactor Theory," Cambridge University Press, Cambridge, Mass., 1965.
(28) S. Dushman, "Vacuum Technique," 2nd ed, John Wiley and Sons, Inc., New York, N. Y., 1962, p 90. Equation 7 is derived from Dushman's eq 2.36 by dividing the pumping speed of the aperture by the vessel volume in liters.
(29) We may note that the escape rate constant is independent of gas pressure. This means that the volume effect treated by, for example, G. M. Harris (*J. Phys. Colloid Chem.*, 51, 505 (1947)) does not apply to VLPP conditions.

rewrite k in terms of the vessel collision number Z_r and the internal surface area of the vessel A_v (cm^2)

$$k = \frac{3.65\delta_p A_v T^{1/2}}{V n_p M_A^{1/2} Z_r} \quad (9)$$

Now

$$\frac{\delta_p}{n_p} = \frac{\delta_q}{n_q} = \frac{f}{(1-f)} \quad (10)$$

where f is the fraction of unimolecular decomposition of A in the reactor.

From eq 5 and 10

$$k = k_{ea}\frac{f}{(1-f)} \quad (11)$$

From eq 9 and 10

$$k = \frac{3.65 A_v T^{1/2}}{Z_r V M_A^{1/2}}\left[\frac{f}{(1-f)}\right] \quad (12)$$

It will be noted that eq 11 and 12 bear a formal similarity to the equations for a stirred flow reactor.[30]

If f' represents the fraction of A disappearing by chemical reaction with B, we can show that

$$k_b(B)_{SS} = \frac{3.65 A_v T^{1/2}[f'/(1-f')]}{Z_r V M_A^{1/2}} \quad (13)$$

Here $f'/(1-f')$ is a direct experimental observable and is equal to δ_r/n_r or δ_s/n_s.

Since our experimental data give $f/(1-f)$ and $f'/(1-f')$ directly, we can immediately use eq 12 and 13 to give first-order and second-order rate constants.

Some experiments are not directly amenable to the foregoing treatment. For example, we may sometimes not be able to measure the relative sensitivities of a parent molecule and its free-radical decomposition products. For such experiments we must measure the absolute flux of parent molecules under the various experimental conditions.

The mass spectrometer signal I_A is closely proportional to the flux of species A. If we denote the constant of proportionality (or sensitivity) by α_A, then (with eq 2)

$$I_A = \alpha_A k_{ea}(A)_{SS} = \frac{N_A k_{ea}\alpha_A}{k + k_{ea} + k_b(B)_{SS}} \quad (14)$$

We can determine α_A by calibration.[32]

In this type of measurement N_A, the mass flow rate, is kept constant and the temperature range is scanned. At low temperatures where no reaction takes place, we observe a signal $I_A^0 = N_A\alpha_A$ (from eq 4) so that we can eliminate N_A and α_A and write

$$\frac{I_A}{I_A^0} = \frac{k_{ea}}{[k + k_{ea} + k_b(B)_{SS}]} \quad (15)$$

(30) Equation 12 can be transformed to eq 10 of ref 31 by the substitutions $k/k_w = b$, $f = B$, and $Z_r = \nu_m$. k_w is the wall-collision frequency where $k_w = 3.65 A_v T^{1/2}/(V M_A^{1/2})$ sec^{-1}.

(31) P. LeGoff, *J. Chim. Phys.*, 359 (1956).

(32) One must correct for the effect of oven temperature on α_A when working with molecular beams. This problem has been studied by O. Osberghaus and R. Taubert, *Z. Physik. Chem.* (Leipzig), **B516**, 264 (1955); H. Ehrhardt and O. Osberghaus, *Z. Naturforsch.*, **13a**, 16 (1958); **15a**, 575 (1960). The mass spectrometer experiments described earlier in this paper were not beam experiments and most of the molecules were cooled to close to ambient temperature prior to entering the ionizer.

Solving for k, the apparent first-order rate constant for decomposition of A, we find

$$k = k_{ea}\left[\left(\frac{I_A^0}{I_A}\right) - 1 - \frac{k_b(B)_{SS}}{k_{ea}}\right] \quad (16)$$

In the absence of any secondary reactions by B, we have

$$k = k_{ea}\left[\left(\frac{I_A^0}{I_A}\right) - 1\right] = k_{ea}\left(\frac{I_A^0 - I_A}{I_A}\right)$$

or, alternatively

$$k = k_{ea}\frac{f}{(1-f)} \quad (17)$$

2. Induction Periods. Two types of induction times must be considered in our system. The first, τ_m, corresponds to a "mixing" time and arises because reactant molecules are introduced at one end of a cylindrical vessel and escape from an orifice at the opposite end. The probability of escape is lower for these molecules than for the average molecule, and one can make a simple estimate that in time τ_m, Z_m collisions are required to bring these molecules to an "average" position in our cell. For a cylinder of length l cm and radius r cm, $Z_m \sim (l/2r)^2$. Z_m is estimated on the basis of a random walk of step size r cm. For our system Z_m is about 4 to 6 and generally negligible.

The second induction period is related to the time τ_i necessary to reach the stationary population of the upper vibrational levels of the reactant molecules. Since internal energies of average reacting molecules are in the range of $40RT$, one would imagine that on the order of at least 40 and possibly $(40)^2$ wall collisions would be required to establish such stationary states.

We can examine the effect of this internal energy relaxation by considering the fate of a number of molecules $V(\Delta A)$ introduced into the reactor at time $t = 0$ in a time interval $\Delta\tau$ which is very short compared to the mean residence time τ_r in the reactor. Note that $\tau_r = 1/(k_{ea} + k)$.

Ignoring the complications of secondary reactions with B, the rate of depletion of the group ΔA in the reactor is given by

$$\frac{-d(\Delta A)}{dt} = (k + k_{ea})(\Delta A) \quad (18)$$

where k is now some monotonic function of time. If we wish to take account of the mixing time τ_m, we can easily do so by saying that k_{ea} is a step function, $k_{ea} = 0$ for $0 \leq t \leq \tau_m$, and $k_{ea} = k_{ea}$ for $t \geq \tau_m$, with $\tau_m = Z_m\tau_w$ where τ_w is the mean time between wall collisions.

Integrating eq 18 between limits 0 and t, we find

$$-\ln\left[\frac{(\Delta A)}{(\Delta A)_0}\right] = k_{ea}(t - \tau_m) + \int_0^t k\,dt \quad (19)$$

$$= k_{ea}(t - \tau_m) + \langle k\rangle t \quad (20)$$

where $\langle k\rangle$ is the average of k over the time interval t and is a function of t as defined by eq 19 and 20.

Now the rate of unimolecular reaction is given by

$$-\left[\frac{d(\Delta A)}{dt}\right]_{chem} = k(\Delta A) \quad (21)$$

and, on eliminating (ΔA) with the aid of eq 20

$$\frac{-1}{(\Delta A)_0}\left[\frac{d(\Delta A)}{dt}\right]_{chem} = k \exp\{-[k_{ea}(t - \tau_m) + \langle k\rangle]\} \quad (22)$$

The total fraction of chemical reaction f which occurs in the group ΔA is obtained by integrating eq 22 between limits $0 \leq t \leq \infty$. We find

$$f = \exp(k_{ea}\tau_m)\int_0^\infty k \exp[-(k_{ea} + \langle k\rangle)t]\, dt \quad (23)$$

This can be integrated if we have an explicit form for $k(t)$. As a simple case which is probably not far from reality, we may assume that k is a step function such that $k = 0$ for $0 < t < \tau_i$ and $k = k$ for $t \geq \tau_i$. τ_i is then an induction time for energy relaxation. Under these conditions f becomes

$$f = \frac{k \exp\{-k_{ea}(\tau_i - \tau_m)\}}{(k_{ea} + k)} = \frac{k/\beta}{(k_{ea} + k)} \quad (24)$$

with $\beta \equiv \exp\{k_{ea}(\tau_i - \tau_m)\}$ and generally $\beta \geq 1$.

Solving for k we find a result similar to eq 11

$$k = \frac{k_{ea} f\beta}{(1 - f\beta)} \quad (25)$$

where $f\beta$ can be interpreted as a corrected fraction of decomposition.

In vessels with very small apertures where $k_{ea}(\tau_i - \tau_m) << 1$, eq 11 and 25 are identical, and we can ignore the induction times. This permits us to solve for k from calculations of k_{ea} (eq 7) and measurement of f. We can then solve for the induction parameters (from eq 24) by measuring f at the same temperatures in a series of vessels of different k_e where $k_e(\tau_i - \tau_m) \approx 1$.

From preliminary results reported here, it appears as though for isopropyl iodide, at about 1000°K, $(\tau_i - \tau_m) \sim 4$ msec in a conditioned quartz vessel. This would correspond to about 80 wall collisions for the average *i*-PrI molecule to pick up about $40RT$ of internal energy. If we assume an oversimple Brownian process of energy exchange between the walls and *i*-PrI molecules, this corresponds to about $4.5RT = 9$ kcal/mole transfer of energy per wall collision, essentially a "strong" collision mechanism.[33]

3. RRK Theory of the Unimolecular Rate Constant k_u. The Rice–Ramsperger–Kassel (RRK) theory of unimolecular reactions assumes that molecules are activated and deactivated by collisions and that a stationary population of vibrationally excited species is produced by these processes together with the process of spontaneous unimolecular decomposition. The rate constant falls off from its high-pressure limit when spontaneous decomposition depletes the upper energy states responsible for reaction faster than collisional deactivation does.

Normally, one studies such effects by measuring the apparent first-order rate constant at fixed temperature but successively lower pressures. In the VLPP technique, the frequency of wall collisions is essentially fixed by the dimensions of the vessel. As one goes to higher and higher temperatures, the rate of spontaneous decomposition increases, and at sufficiently high temperatures all unimolecular reactions will fall off from their high-pressure limits.

(33) G. H. Kohlmaier and B. S. Rabinovitch, *J. Chem. Phys.*, **38**, 1692 (1963).

For an arbitrary reactant molecule A, the RRK scheme is[34]

$$\text{wall} + A \underset{k_d}{\overset{k_a}{\rightleftharpoons}} A^* + \text{wall}$$

$$A^* \xrightarrow[k_r]{} \text{products} \quad (26)$$

Here k_a and k_d are rate constants for vibrational energy exchange at the wall, and k_r is the specific decomposition rate of a critically energized molecule with internal energy $E \geq E^*$, the activation energy for reaction at 0°K. The observed apparent first-order rate constant k is then

$$k = \int_{E^*}^\infty \frac{k_a k_r}{k_d + k_r}\, dE \quad (27)$$

Using the classical RRK forms for k_r and k_a/k_d, it can be shown that the integrand in eq 27 has a simple sharp maximum at $E = E_m$ where $E^* \leq E_m \leq E^* + (n - 1)RT$, and n is the effective number of classical oscillators in the molecule A. If the half-width of the integrand is ΔE_m around the maximum, then we can write

$$k = \frac{k_a(E_m)k_r(E_m)(\Delta E_m)/RT}{[k_d(E_m) + k_r(E_m)]} \quad (28)$$

It can be further shown that this maximum occurs very close to the value of E_m that makes $k_d(E_m) \sim k_r(E_m)$, so that eq 28 becomes

$$k \approx \left(\frac{k_a}{2}\right)\frac{(\Delta E_m)}{RT} = \left(\frac{k_a}{k_d}\right)\left(\frac{k_d}{2}\right)\left(\frac{\Delta E_m}{RT}\right) = \frac{1}{2}P(E_m)k_d\frac{\Delta E_m}{RT} \quad (29)$$

where $P(E_m) = k_a/k_d$ is the probability of finding a molecule of internal energy E_m in a system at equilibrium. It is given classically by

$$P(E_m) = \frac{1}{(n-1)!}\left(\frac{E_m}{RT}\right)^{n-1}\exp\left(\frac{-E_m}{RT}\right) \quad (30)$$

Now $k_d(E_m)$ can be written as $\lambda_d k_w$, where k_w is the frequency of wall collisions, typically $\sim 10^{4.5}$ sec^{-1} in our system, and λ_d is the probability that a molecule with internal energy E_m will, on a wall collision, lose enough of this energy that it is not capable of reacting in $10^{-4.5}$ sec. The amount of energy required is probably of the order of $2RT$ and λ_d is probably of the order of 1. Thus we can set

$$k_r(E_m) = k_d(E_m) \cong k_w \quad (31)$$

while from the RRK theory

$$k_r(E_m) = A\left(\frac{E_m - E^*}{E_m}\right)^{n-1} \quad (32)$$

where A is the Arrhenius A factor in sec^{-1}. From eq 31 and 32

$$1 - \frac{E^*}{E_m} = \left(\frac{k_w}{A}\right)^{1/(n-1)} \quad (33)$$

or

$$\frac{E^*}{E_m} = 1 - \left(\frac{k_w}{A}\right)^{1/(n-1)} \quad (34)$$

(34) S. W. Benson, "Foundations of Chemical Kinetics," McGraw-Hill Book Co., Inc., New York, N. Y., 1960, Chapter XI.

Thus if we know or can choose a value of n and A we can calculate the ratio E^*/E_m for our system.

Having calculated the ratio (E^*/E_m), one then uses eq 29 and 30 with $\Delta E_m/RT \sim (n-1)^{1/2}$ to calculate E_m at any given temperature.[35] This is done numerically, explicit solutions not being possible.

With Stirling's approximation for $(n-1)!$ we have from eq 29 and 30

$$k = \frac{k_w}{2\sqrt{2\pi}}\left[\frac{eE_m}{(n-1)RT}\right]^{n-1}\exp\left(-\frac{E_m}{RT}\right) \quad (35)$$

which permits us to solve for E_m from the observed value of k and the appropriate value of n.

When the high-pressure Arrhenius parameters A and E^* are known, as is often the case, n is the only unknown parameter and it can be determined accurately.

We have used eq 35 in our theoretical estimates for the rate of decomposition of *i*-PrI.

(35) This approximation for ΔE_m is obtained by use of the method of steepest descents for the integration of eq 29.

A Nuclear Magnetic Resonance Study of Steric Effects in *cis*- and *trans*-1,4-Dichloro-2-butene[1]

Harry G. Hecht[2] and Bob L. Victor

Contribution from the University of California, Los Alamos Scientific Laboratory, Los Alamos, New Mexico, and the Department of Chemistry, Texas Technological College, Lubbock, Texas. *Received December 16, 1966*

Abstract: The 60-Mc nmr spectra of *cis*- and *trans*-1,4-dichloro-2-butene are reported and analyzed. A population analysis based upon the observed vicinal couplings indicates that the steric interaction between $-CH_2Cl$ groups in the *cis* isomer is at least 170 cal mole^{-1} larger when the chlorine atom is oriented *trans* with respect to the adjacent vinyl proton.

The nuclear spin–spin coupling between vicinal protons in HC–CH groups of ethane and ethylene-type molecules has been found to be dependent upon the dihedral angle.[3] Since internal rotational energy barriers about carbon–carbon single bonds are low, only an average coupling is observed in many cases, but such an average can still be useful to determine which is the more stable rotamer.

The analysis of the complex nmr spectra of *cis*- and *trans*-1,4-dichloro-2-butene was undertaken since the coupling constants obtained from these spectra can be used to infer the conformation of the CH_2Cl groups about the carbon–carbon single bonds. Our primary objective was to see if we could determine the extent of the steric interaction of these groups in the *cis* compound.

The basis for our conformational study rests upon the following considerations. Figure 1 shows the anticipated stable conformation of *trans*-1,4-dichloro-2-butene.[4-6] It is assumed that in this case a certain average vicinal coupling between the methyl protons (H_a) and the adjacent vinyl proton (H_b) will be observed, the magnitude of which is determined by the energy difference between the conformation of Figure 1 and others obtained by rotations about the carbon–carbon single bonds. If the same *trans* orientation of an H_a proton with respect to the adjacent H_b proton persisted in the *cis* isomer, we would expect to observe a rather strong steric interaction between the H_a protons of the different $-CH_2Cl$ groups. Of course with the chlorine atoms *trans* with respect to H_b, the steric effect would be even more pronounced. Because of these interactions, conformational stability requirements are altered, and these changes should be reflected in the average proton couplings observed.

This unsaturated system may be regarded as an allylic system, since there is spin–spin coupling between protons separated by one double bond and three single bonds, and also as a homoallylic system, where the coupling between protons is over five bonds with the protons symmetrically placed about the carbon–carbon double bond, *i.e.*, H—C—C=C—C—H.[7]

Karplus,[8] through a valence bond treatment, has had most success in correlating experimental results with theoretical calculations, with respect to both the sign and magnitude of couplings in allylic and homoallylic systems. The proposed mechanism involves hyperconjugation determined by σ–π configuration interaction.

From the theoretical point of view, the allylic coupling constants are negative in sign with the coupling being transmitted mainly through the π-electron system.[8] The magnitudes of the allylic coupling constants have been found to vary between 0 and 3 cps.[9] These coupling constants attain a maximum of approximately 3 cps when the azimuthal angle is 90°, and a minimum when the azimuthal angle is 0 or 180°.

(1) Based in part on work performed under the auspices of the U. S. Atomic Energy Commission.
(2) Author to whom inquiries should be addressed: University of California, Los Alamos Scientific Laboratory, Los Alamos, N. M. 87544.
(3) M. Karplus, *J. Chem. Phys.*, 30, 11 (1959).
(4) M. Barfield and D. M. Grant, *J. Am. Chem. Soc.*, **85**, 1899 (1963).
(5) H. J. M. Bowen, A. Gilchrist, and L. E. Sutton, *Trans. Faraday Soc.*, **51**, 1341 (1955).
(6) A. A. Bothner-By and H. Günther, *Discussions Faraday Soc.*, **34**, 127 (1962).
(7) S. Sternhell, *Rev. Pure Appl. Chem.*, **14**, 15 (1964).
(8) M. Karplus, *J. Chem. Phys.*, **33**, 1842 (1960).
(9) F. A. L. Anet, *Can. J. Chem.*, **39**, 2262 (1961).